J. of Supercritical Fluids 58 (2011) 158–167

Contents lists available at ScienceDirect

The Journal of Supercritical Fluids

journal homepage: www.elsevier.com/locate/supflu

Solid-state supercritical CO_2 foaming of PCL and PCL-HA nano-composite: Effect of composition, thermal history and foaming process on foam pore structure

A. Salerno[a,b,*], E. Di Maio[c], S. Iannace[b], P.A. Netti[a,c]

[a] Interdisciplinary Research Centre on Biomaterials (CRIB) and Italian Institute of Technology (IIT), Piazz.le Tecchio 80, 80125 Naples, Italy
[b] Institute of Composite and Biomedical Materials, National Research Council (IMCB-CNR), Piazz.le Tecchio 80, 80125, Naples, Italy
[c] Department of Materials and Production Engineering, University of Naples Federico II, Piazz.le Tecchio 80, 80125 Naples, Italy

ARTICLE INFO

Article history:
Received 1 March 2011
Received in revised form 6 May 2011
Accepted 17 May 2011

Keywords:
Solid-state foaming
Poly(ε-caprolactone)
Scaffold
Supercritical CO_2

ABSTRACT

In this work we investigated the solid-state supercritical CO_2 ($scCO_2$) foaming of poly(ε-caprolactone) (PCL), a semi-crystalline, biodegradable polyester, and PCL loaded with 5 wt% of hydroxyapatite (HA) nano-particles.

In order to investigate the effect of the thermal history and eventual residue of the crystalline phase on the pore structure of the foams, samples were subjected to three different cooling protocols from the melt, and subsequently foamed by using $scCO_2$ as blowing agent. The foaming process was performed in the 37–40 °C temperature range, melting point of PCL being 60 °C. The saturation pressure, in the range from 10 to 20 MPa, and the foaming time, from 2 to 900 s, were modulated in order to control the final morphology, porosity and pore structure of the foams and, possibly, to amplify the original differences among the different samples.

The results of this study demonstrated that by the $scCO_2$ foaming it was possible to produce PCL and PCL-HA foams with homogeneous morphologies at relatively low temperatures. Furthermore, by the appropriate combination of materials properties and foaming parameters, we prepared foams with porosities in the 55–85% range, mean pore size from 40 to 250 μm and pore density from 10^5 to 10^8 pore/cm^3. Finally, we also proposed a two-step depressurization foaming process for the design of bi-modal and highly interconnected foams suitable as scaffolds for tissue engineering.

1. Introduction

Polymeric foams are multi-phase materials characterized by a solid continuous matrix surrounding a gaseous phase. The possibility of combining the properties of a continuous matrix and gas voids in a great variety of pore structures is a powerful tool in the materials industry and research [1]. In particular, depending on the field of application, foams may be rigid or flexible, may possess low or high densities, as well as closed or interconnected pores with different size and shape distributions [1].

In the past years, the development of biodegradable foams and environmentally friendly foaming processes has been a key point for the design of porous materials suitable for several applications, such as acoustic and thermal insulation, as well as tissue engineering (TE) scaffolds [1–6].

Among the environmentally friendly foaming processes that have been developed and successfully implemented to produce biodegradable foams, supercritical CO_2 ($scCO_2$) foaming has recently received great emphasis [2–8]. Indeed, CO_2 is environmentally friendly, non-flammable, and inexpensive [2,3], while $scCO_2$ foaming may be applied to a large class of biodegradable polymers, ranging from synthetic polyesters [3,4] to natural materials such as thermoplastic proteins and saccharides [5,6], as well as their combination [7,8]. Furthermore, the low $scCO_2$ temperature (31.1 °C) and pressure (7.4 MPa), in combination with the non-toxic properties of CO_2, may offer the possibility to process biodegradable materials and heat labile molecules at room temperature by the so called "solid-state" foaming [4,8–11]. This technological feature is extremely important, especially in the pharmaceutical and biomedical fields, because of the need to preserve the chemical and bioactive properties of biomaterials and molecular cues.

The architecture of the pore structure of porous materials prepared via the $scCO_2$ foaming may be fine controlled through the proper selection of the processing conditions, mainly the saturation pressure, the foaming temperature and the depressurization time [1,3–7]. In the case of composite materials, the foaming process can be also controlled appropriately by the selection of the

* Corresponding author at: Interdisciplinary Research Centre on Biomaterials (CRIB) and Italian Institute of Technology (IIT), Piazz.le Tecchio 80, 80125 Naples, Italy. Tel.: +39 0817682536.
E-mail address: asalerno@unina.it (A. Salerno).

0896-8446/$ – see front matter © 2011 Elsevier B.V. All rights reserved.
doi:10.1016/j.supflu.2011.05.009

type and concentration of the filler, therefore giving an additional degree of freedom in the design of the porous network of the foams [3,12,13].

Poly(ε-caprolactone) (PCL) is a hydrophobic, semi-crystalline biodegradable and biocompatible polymer [3,13]. The exceptional thermal stability and blend-compatibility of PCL, coupled with its low melting point (59–64 °C), have stimulated increasing interest in its use for applications such as packaging, loose-fillers, as well as biomedical devices and scaffolds [14].

In the past years, the solid-state $scCO_2$ foaming of completely amorphous polymers, such as polystyrene, poly(DL-lactic acid) and poly(lactic co-glycolic acid), have been widely investigated and successfully implemented to produce homogeneous foams with controlled pore structures [9–11]. Conversely, it has been reported that the solid-state $scCO_2$ foaming of semi-crystalline polymers, such as PCL, resulted in foams with inhomogeneous pore structures and, often reduced processing window in terms of foaming capability was observed [15,16]. These results have been mainly ascribed to the high crystalline fraction of PCL (60–70%) that induced the presence of non-plasticized crystal regions that may hinder the uniformity of the foams and, eventually, impede foaming at all [16]. To overcome this limitation, research efforts have been thus focused on the development of binary mixtures made of $scCO_2$ and co-solvents, such as ethanol and acetone, able to improve the solubility of $scCO_2$ in PCL [4,17]. Although this approach allowed the fabrication of PCL foams with more homogeneous pore structures and improve foamability, the use of organic solvents may be potentially detrimental for applications requiring the incorporation of bioactive molecules within the foams or the interaction with biological entities, such as in the case of TE scaffolds [11].

The present work aims to provide new insights about the solid-state $scCO_2$ foaming of PCL and PCL loaded with HA nano-particles. The concern here, is that $scCO_2$ could induce a gas concentration-induced melting (although at temperatures well below 60 °C) of our samples, and that this phenomenon could be dependent on the imposed thermal history. As a direct consequence, PCL and PCL-HA foams with different pore structures may be achieved as a function of the thermal history of the starting samples. The selection of the HA as inorganic filler was conducted to open to the possible design of hybrid osteo-inductive scaffolds for hard TE applications [7,12].

The effect of the HA particles and cooling process on the thermal properties of the materials was investigated by scanning calorimetric analysis, and the results were correlated to the pore structure features of the resulting foams. Finally, a two-step depressurization solid-state foaming process was proposed as a suitable approach for the design of PCL and PCL-HA nano-composite scaffolds with bi-modal pore size distributions and high degree of pore interconnectivity.

2. Materials and methods

2.1. Materials

PCL (M_W = 65 kDa) was purchased from Sigma–Aldrich (Italy). HA nano-particles (Berkeley Advanced Biomaterials Inc., Berkeley, CA) with 100 nm mean size were selected for the preparation of the PCL-HA composites. CO_2 with purity grade of 99.99% (Air liquide, Italy) was used as blowing agents for gas foaming experiments.

2.2. Methods

2.2.1. Samples preparation

A PCL-HA nano-composite containing 5 wt% of inorganic particles was prepared by using an internal mixer (Rheomix® 600, Haake, Germany) controlled by a measuring drive unit (Rheocord® 9000, Haake, Germany). PCL pellets were first melted and, subsequently, the HA particles were added into the mixing chamber and mixed with the polymer at 70 °C, 100 rpm for 10 min. The as obtained sample was extracted from the mixer and compression moulded to produce 200 μm-thick films, by a hot press (P 300 P, Collin, Germany) at 80 °C and at 10 MPa. Three different cooling histories were used to cool down the molten samples from 80 to 25 °C: (1) the molten material was quenched by soaking in liquid N_2 (fast cooling rate); within the press, the material was allowed to cool to room temperature in (2) 2 min (intermediate cooling rate) and (3) 15 min (slow cooling rate). Neat PCL was subjected to the same processes for proper comparison. All of the samples were then stored at −30 °C to avoid polymer re-crystallization before further processing.

2.2.2. Thermal characterization of the samples before and after the isothermal $scCO_2$ treatment

It has been reported that solubilised $scCO_2$ may depress characteristic temperatures (melting as well as glass transition) of polymers, a phenomenon generally referred to as plasticizing effect [18–20]. The differential scanning calorimetry (DSC) was used to assess the effect of the thermal history and $scCO_2$ solubilization on the melting properties of PCL and PCL-HA nano-composite. Before the analysis, the samples were subjected to an isothermal $scCO_2$ treatment. The process was conducted in a high-pressure vessel (HiP, Pennsylvania, USA) [13] and the $scCO_2$ solubilized at 37 °C and 20 MPa for 1.5 h. When opening the vessel, to minimize polymer foaming during depressurization, the pressure vessel was cooled down to 5 °C and CO_2 evacuated very slowly (2 h approximately). The as obtained samples were tested on a DSC Q1000 (TA Instruments, USA) in the temperature range from 10 to 80 °C and at a scanning rate of 10 °C/min under inert atmosphere. The same tests were performed on the untreated PCL and PCL-HA samples. The melting peak temperature (T_{PEAK}), heat of fusion (ΔH_F) and starting melting temperature (T_0) of the PCL and PCL-HA before and after isothermal $scCO_2$ treatment were determined by the DSC tests.

2.2.3. Solid-state $scCO_2$ foaming

Foaming experiments were carried out on disc-shaped samples obtained by overlapping five samples (200 μm-thick and 10 mm in diameter) characterized by the same composition and thermal history. The solubilisation of the $scCO_2$ was performed at saturation pressures and temperatures in the range from 10 to 20 MPa and from 37 to 40 °C, respectively, while the solubilisation time was varied from 1.5 to 12 h. Foaming was induced by quenching the pressure to the ambient. Three different foaming times, in the range from 2 to 900 s and obtained by selecting different gas-discharge capillaries with appropriate length and diameter of the $scCO_2$ release system, were used to control the pore structure features of the foams [13]. A two-step depressurization process [21] was also investigated to prepare highly interconnected bi-modal PCL and PCL-HA foams for TE. In particular, the fast cooled samples were solubilised at 37 °C and 20 MPa for 1.5 h and, subsequently, the pressure was slowly released to an intermediate pressure of 9 MPa. After the re-equilibration of the temperature of the system to 37 °C, the pressure was finally quenched to the ambient very fast to allow for the formation of a bi-modal pore structure.

2.2.4. Foams characterization

The morphology of the foams was assessed by scanning electron microscopy (SEM). The samples were cross-sectioned, gold sputtered and analyzed by SEM (S440, LEICA, Germany).

The density of the foams (ρ_F) was determined from the mass and the volume measurements. The mass was measured by using a high accuracy balance (10^{-4} g, AB104-S, Mettler Toledo, Italy) while the volume determined by displacement method (ASTM

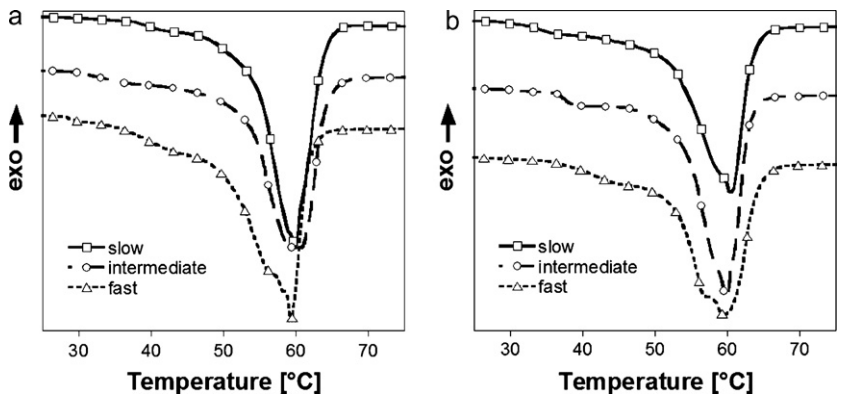

Fig. 1. DSC heating curves of the non-isothermal crystallized (a) PCL and (b) PCL-HA nano-composite samples.

D1622-03). The porosity of the foams was then assessed by the following equation [3]:

$$\text{Porosity}\ \ \% = \left[1 - \left(\frac{\rho_F}{\rho_P}\right)\right] \times 100$$

where ρ_P is the density of the polymeric phase (pure PCL or PCL-HA composite).

The mean pore size and the pore size distribution of the foams were evaluated by image analysis. One hundred pores for each sample were analyzed by using the "particle analysis" tools of the Image J software pack, that enable to assess the area of each pores. The pore diameter was then calculated with the hypothesis of spherical shape pores and, by correcting the as obtained values by the factor $4/\pi$, according to the ASTM D3576.

The number of pores per cm^3 of the foam (N_f) was assessed by using the equation [1]:

$$N_f = \frac{\text{porosity}}{[(\pi/6) \times (\text{pore diameter})^3]}$$

3. Results and discussion

3.1. Thermal characterization

The thermal properties of semi-crystalline polymers have a great impact on their foaming behaviour. In this context, the crystallinity plays a major role in foaming processing through its effects on both cell nucleation mechanisms and cell growth. Taking into the account this aspect, in this work we investigated the melting behaviour of the PCL and PCL-HA nano-composite as a function of the thermal history, before and after the $scCO_2$ treatment.

The DSC curves of the first heating scans for the non-isothermally crystallized PCL and PCL-HA films before and after the $scCO_2$ treatment at 37 °C, 20 MPa for 1.5 h are shown in Figs. 1 and 2, respectively. The results of the DSC tests are summarized in Table 1. As shown in Fig. 1a and b, before $scCO_2$ treatment, the increase of the cooling rate resulted in the increase of ΔH_F for both PCL and PCL-HA. Although it has been frequently reported an opposite trend, this effect demonstrated that extensive PCL crystallization occurred also at very high cooling rates, even if in this case smaller crystalline domains may be expected, as suggested by the marked endothermic shoulders on the DSC curves visible near 40 °C for the fast cooled samples. Minor differences were conversely observed for T_0 and T_{PEAK}, characterized by values close to 60 °C for all of the samples prepared.

Significant changes in the thermal properties of the samples were observed after the $scCO_2$ treatment. In particular, all of the $scCO_2$-crystallized samples evidenced higher T_{PEAK} values if compared to the untreated ones (Table 1). This effect was more marked for the PCL and PCL-HA samples quenched in liquid N_2 (fast), for which T_{PEAK} increased from 59.8 to 64.7 °C and from 59.6 °C to 63 °C, respectively. Interestingly, the DSC scan of the slowly cooled PCL sample after the exposure to the $scCO_2$, reported in Fig. 2a, showed a double melting peak, characterized by peak temperatures equals to 58.8 and 62.4 °C. The $scCO_2$ treatment also increased the values of ΔH_F and T_0 of all of the samples.

As previously discussed, there are several studies reporting that, when in contact with $scCO_2$, PCL may undergo to partial or complete melting at temperatures well below its melting point at ambient pressure [18–20]. For instance, Kiran and co-workers showed that the saturation of $scCO_2$ at 21 MPa and 35 °C for 30 min induced the melting of PCL, as shown by both thermal and micro-structural characterizations [20]. In agreement with the results of our study,

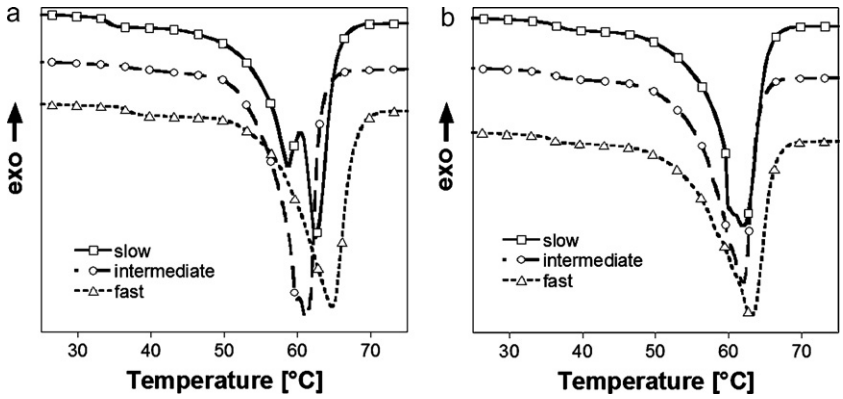

Fig. 2. DSC heating curves of the non-isothermal crystallized (a) PCL and (b) PCL-HA nano-composite samples after isothermal $scCO_2$ treatment at 37 °C and 20 MPa for 1.5 h.

Table 1
DSC results of the PCL and PCL-HA samples before and after the $scCO_2$ treatment at 37 °C and 20 MPa for 1.5 h.

	Before CO_2 treatment Cooling			After CO_2 treatment Cooling		
	Fast	Intermediate	Slow	Fast	Intermediate	Slow
PCL						
ΔH_F (W/g)	85.8	80.3	78.8	88.1	86.4	92.9
T_0 (°C)	53.0	52.8	53.8	56.3	57.0	59.5
T_{PEAK} (°C)	59.8	60	59.9	64.7	61.2	58.8; 62.4
PCL-HA						
ΔH_F (W/g)	84.9	83.8	83.4	85.9	87.5	93.8
T_0 (°C)	52.4	53	53.2	58.7	57.3	59
T_{PEAK} (°C)	59.6	59.8	60	63	62.1	62

they also reported the shifting of the melting peak to higher temperatures after the $scCO_2$ treatment and, in such cases, the presence of a double melting peak, as observed in the case of the slowly cooled PCL sample [20]. The observed differences in the melting behaviour with respect to the thermal history may therefore arise from the diverse melting and subsequent re-crystallization of the polymer after the $scCO_2$ sorption–desorption process. Although the DSC data do not allow for the specific analysis of the crystalline structure of the samples, they demonstrated that $scCO_2$ treated sample's melting was promoted by the increase of the cooling rate of the starting materials. This effect may be explained by the fact that the increase of the cooling rate produced materials with smaller crystallites and, in such cases for samples "instantaneous" quenched in liquid N_2, the formation of meta-stable low melting crystalline forms was also observed [1,22]. As a direct consequence, with the increase of the cooling rate the ability of the $scCO_2$ to diffuse within the crystalline region and plasticize/melt the polymer increased. Then, after the $scCO_2$ desorption, a higher crystalline fraction characterized by larger crystallites were obtained in the case of the fast cooled samples, as evidenced by the shift of the melting peaks to higher temperatures. Nevertheless, these aspects will be the object of a more detailed investigation in future works. It is important to point out, however, that thermal analysis indicated that $scCO_2$ treatment does induce relevant changes in the structure of the materials, but does not cancel their thermal histories, as demonstrated by the differences among the different materials evidenced in Fig. 2. Therefore, a different foaming behaviour may be achieved as a function of the thermal histories, as will be described in detail in the following section.

3.2. Solid-state $scCO_2$ foaming

3.2.1. Effect of the processing parameters on the pore structure of the PCL and PCL-HA foams

The control of the pore structure features of porous materials prepared via the $scCO_2$ foaming process is strongly dependent on the proper selection of the operating conditions with respect to the specific system under investigation [1–9]. For instance, temperature and pressure define the amount of CO_2 solubilised within the material, that has an important role on pores nucleation and growth [1,2,9]. Furthermore, when in contact with $scCO_2$, semi-crystalline structure of the polymer may be subjected to some modifications again dependent on temperature and pressure [9,15,16] and, by the eventual presence of heterogeneous nucleation sites, which may be the HA particles and/or the crystallites [13]. Finally, the foaming step, that involves the nucleation and growth of CO_2 bubbles within the plasticized polymer, is controlled by the polymer/gas de-mixing process, that is mainly dependent on the gas concentration and temperature profile of the system [1,3–5]. These parameters also affect the viscosity of the polymer/gas solution and, therefore pores coalescence and interconnectivity [1,3–5].

In this work we performed a systematic investigation on the material/processing/pore structure properties of PCL and PCL-HA

#	Saturation time [h]	Saturation pressure [MPa]	Saturation temperature [°C]	Foaming time [s]	PCL foams			PCL-HA foams		
					slow	Intermed	fast	slow	intermed	fast
1	1.5	20	37	15	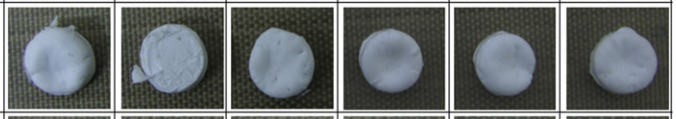					
2	12	10	37	15	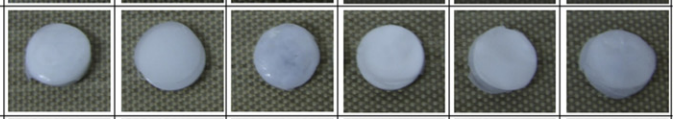					
3	1.5	10	40	15	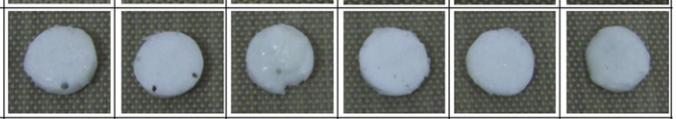					
4	1.5	20	37	2	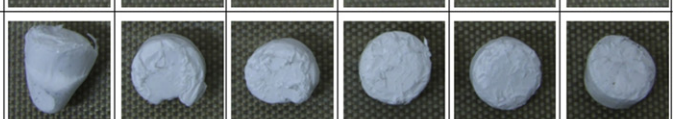					
5	1.5	20	37	900	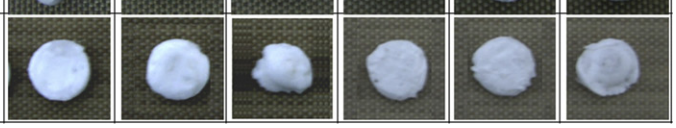					

Fig. 3. Processing conditions used during the solid-state foaming experiments and optical images of the resulting foams.

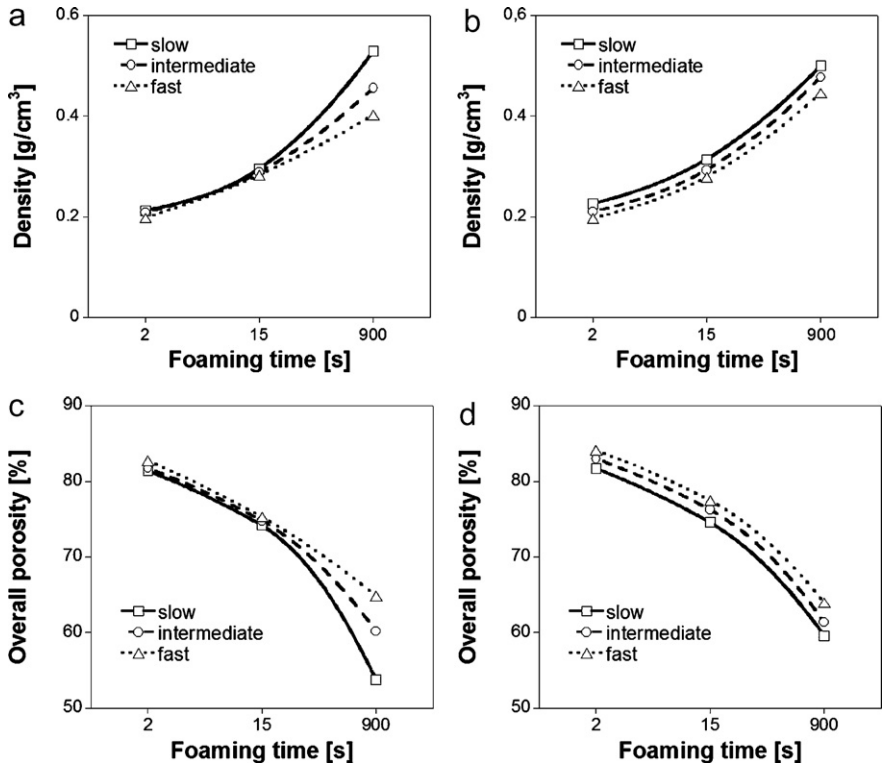

Fig. 4. Density and porosity of the foams as a function of the thermal history and foaming time: (a) and (c) PCL; (b) and (d) PCL-HA.

nano-composite foams prepared by the solid-state $scCO_2$ foaming. Fig. 3 reports the experimental conditions that were used during the foaming tests and the images of the resulting foams. All of the tests were performed at saturation and foaming temperatures below or equal to 40 °C, which is considered suitable for possible incorporation of heat labile molecules within the foams, as previously mentioned [11].

A first set of foaming test (#1–3) was used to tune the different combinations of saturation temperature, pressure and time to achieve suitable foams. In fact, for example, when the saturation step was performed at 10 MPa and 37 °C for 12 h (#2), the different layers composing the starting sample were still visible after foaming, indicating poor blowing agent solubilisation and polymer plasticization. Conversely, uniform foamed samples, indicating extensive melting of the layers, were obtained at a saturation pressure of 20 MPa, even if saturation time was 1.5 h (#1). These results are in agreement with the DSC data of Fig. 2, suggesting the extensive melting of the polymer at the saturation pressure of 20 MPa. To evaluate the possibility to process the materials at a lower pressure, we increased the saturation and foaming temperatures from 37 to 40 °C (#3 of Fig. 3), while keeping the pressure to 10 MPa. Although after the process it was not possible to distinguish the different layers of the sample, in this condition foaming was negligible, as it may be observed from pictures in Fig. 3. This effect was probably due to the depleted blowing agent solubilisation and polymer plasticization at the saturation pressure of 10 MPa and for a saturation time of 1.5 h. Taking into the account all of these results, we performed further foaming tests keeping the saturation temperature and pressure to 37 °C and 20 MPa, respectively, and selecting a fast (2 s, test #4) or a slow (900 s, test #5) depressurization time. The images of the samples processed at different depressurization times showed that the expansion ratio increased with the decrease of the foaming time, and the highest foaming was achieved when the depressurization time was equal to 2 s (#4). Interestingly, at a fixed foaming time, the expansion ratio of the PCL and PCL-HA samples was found to be dependent on their thermal history and, in particular, foaming increased with the decrease of the cooling time (Fig. 3). This result is ascribable to the enhanced melting of the samples with the increase of the cooling rate (Fig. 2). Indeed, the crystalline structure increased the stiffness of the polymeric matrix and, therefore, decreased samples foaming was observed with the increase of the cooling time. To better investigate these phenomena, in the following we performed a detailed morphological and micro-structural characterization of the PCL and PCL-HA foams as a function of the thermal history and time of depressurization and prepared at 20 MPa and 37 °C.

Fig. 4 reports the density and resulting porosities of the PCL and PCL-HA foams as a function of the depressurization time and thermal history. In agreement with the images of Fig. 3, we observed that the density of the foams increased with the increase of the foaming time from 2 to 900 s (Fig. 4a and b). This effect was particularly evident for the slowly cooled PCL sample, for which the density increased from 0.20 to 0.53 g/cm^3 when foaming time increased from 2 to 900 s. Interestingly, at a foaming time of 900 s the PCL films quenched in liquid N_2 (fast) produced a foam with a 40% lower density, if compared to the slowly cooled one. Opposite trends were observed in the case of the porosity of the foams, with the highest porosity value, equal to 82%, achieved in the case of the PCL foam prepared at a depressurization time of 2 s (Fig. 4c). Lower porosity values, in the range from 55 to 65%, were conversely achieved when depressurization was performed for 900 s. The decrease of the porosity with the increase of the foaming time was more marked for the slowly cooled PCL sample, characterized by a 30% porosity decrease from 2 to 900 s of depressurization (Fig. 4c). Similar results were obtained for the PCL-HA nano-composite, indicating a minor influence of the inorganic filler on the density and porosity of the foams.

The increase of the density of the foams as a function of the depressurization time was also reported by Xu and co-workers for the solid-state foaming of PCL, performed at 40 °C and with

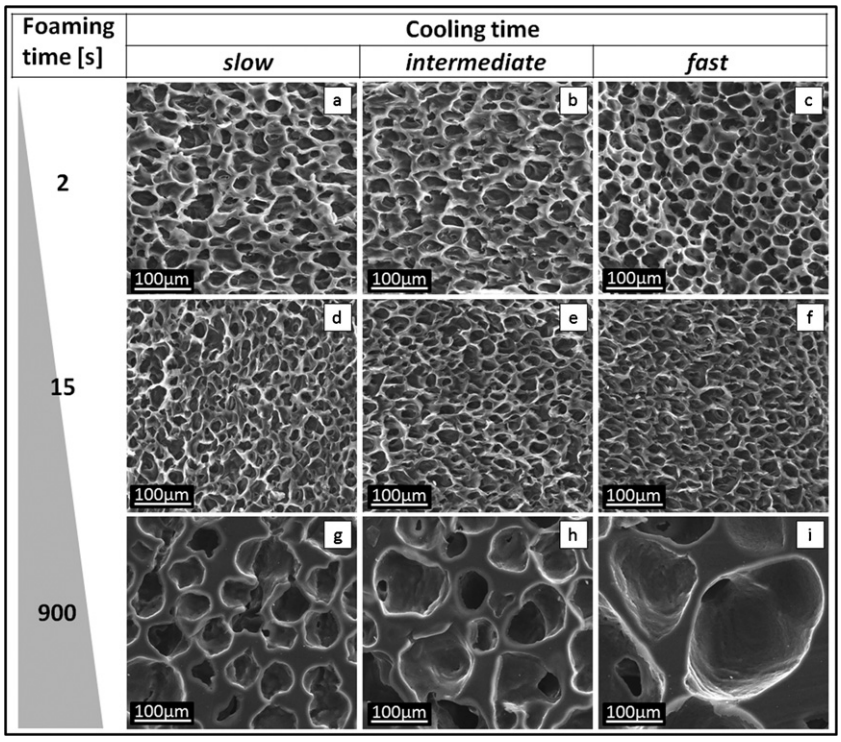

Fig. 5. SEM microscope images of the cross-sections of the PCL foams evidencing the effect of the thermal history and foaming time on the morphology of the samples.

depressurization times up to 300 s [15]. In their work the authors attributed this effect to the increased contraction of the pores with the increase of the depressurization time. Furthermore, our results indicated that foaming was also strongly affected by the thermal history of the starting materials. This effect may be ascribed to the different crystallization of the polymer as a function of the non-isothermal cooling [1]. Recently Xu et al. investigated the solid-state $scCO_2$ foaming of polypropylene, evidencing that the crystalline structure acts in synergy with the depressurization time in controlling pores nucleation and growth within semi-crystalline polymers [23]. In particular, in agreement with our results, they evidenced that, at the saturation pressure of 25 MPa, the increase of the depressurization time decreased the foam volume expansion ratio [23].

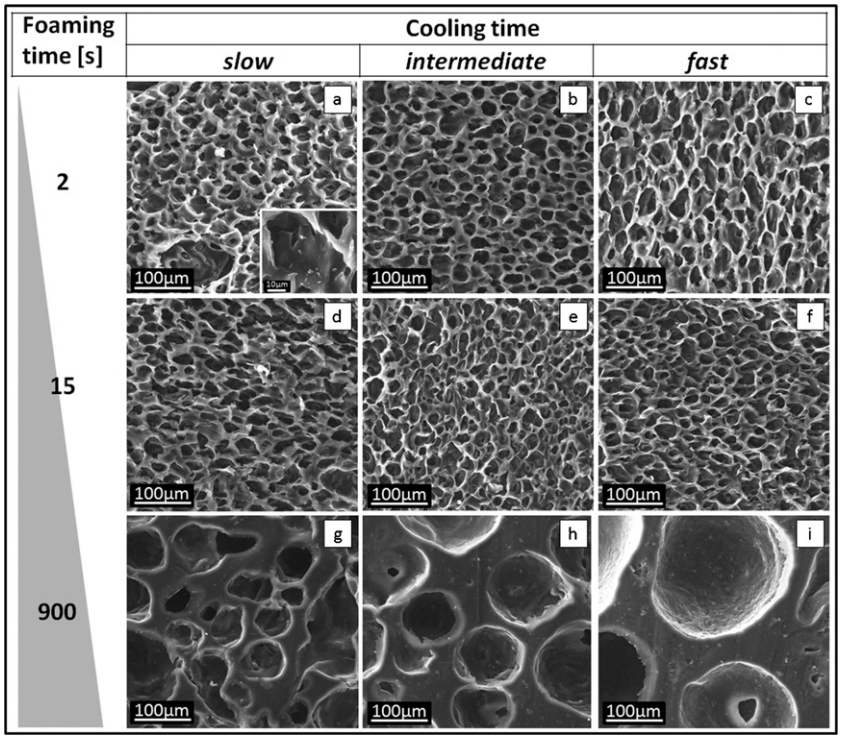

Fig. 6. SEM microscope images of the cross-sections of the PCL-HA foams evidencing the effect of the thermal history and foaming time on the morphology of the samples.

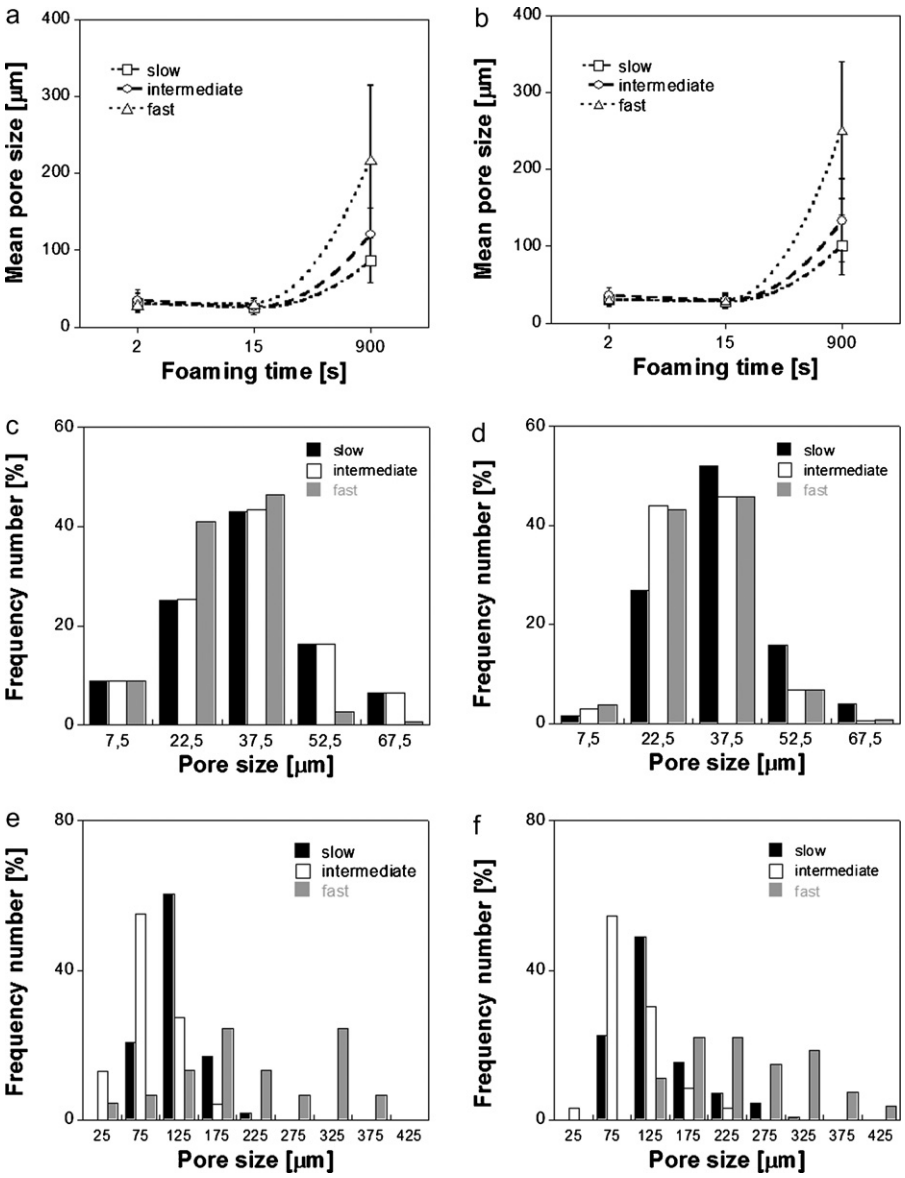

Fig. 7. Effect of the thermal history and foaming time on the mean pore sizes (a) and (b) and pore size distributions (c–f) of the PCL (left column) and PCL-HA (right column) foams. Figures (c) and (d) are related to a foaming time equal to 2 s, while figures (e) and (f) for a foaming time of 900 s.

Figs. 5 and 6 reported the morphology of PCL and PCL-HA foams as a function of the thermal history and depressurization time. As shown, all of the samples were characterized by rather homogeneous morphologies. However, significant differences were observed with respect to the different processing conditions. In particular, the pore size increased with the increase of the depressurization time, with the PCL and PCL-HA samples prepared at the depressurization time of 900 s that were charac-

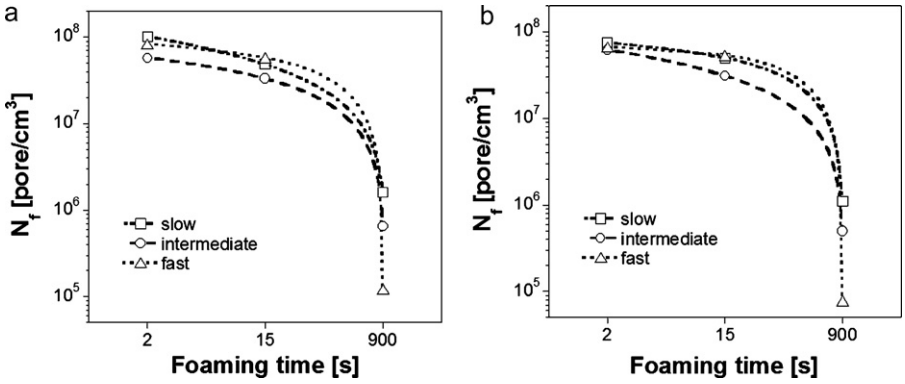

Fig. 8. Pore density, N_f, of the (a) PCL and (b) PCL-HA foams as a function of the thermal history and foaming time.

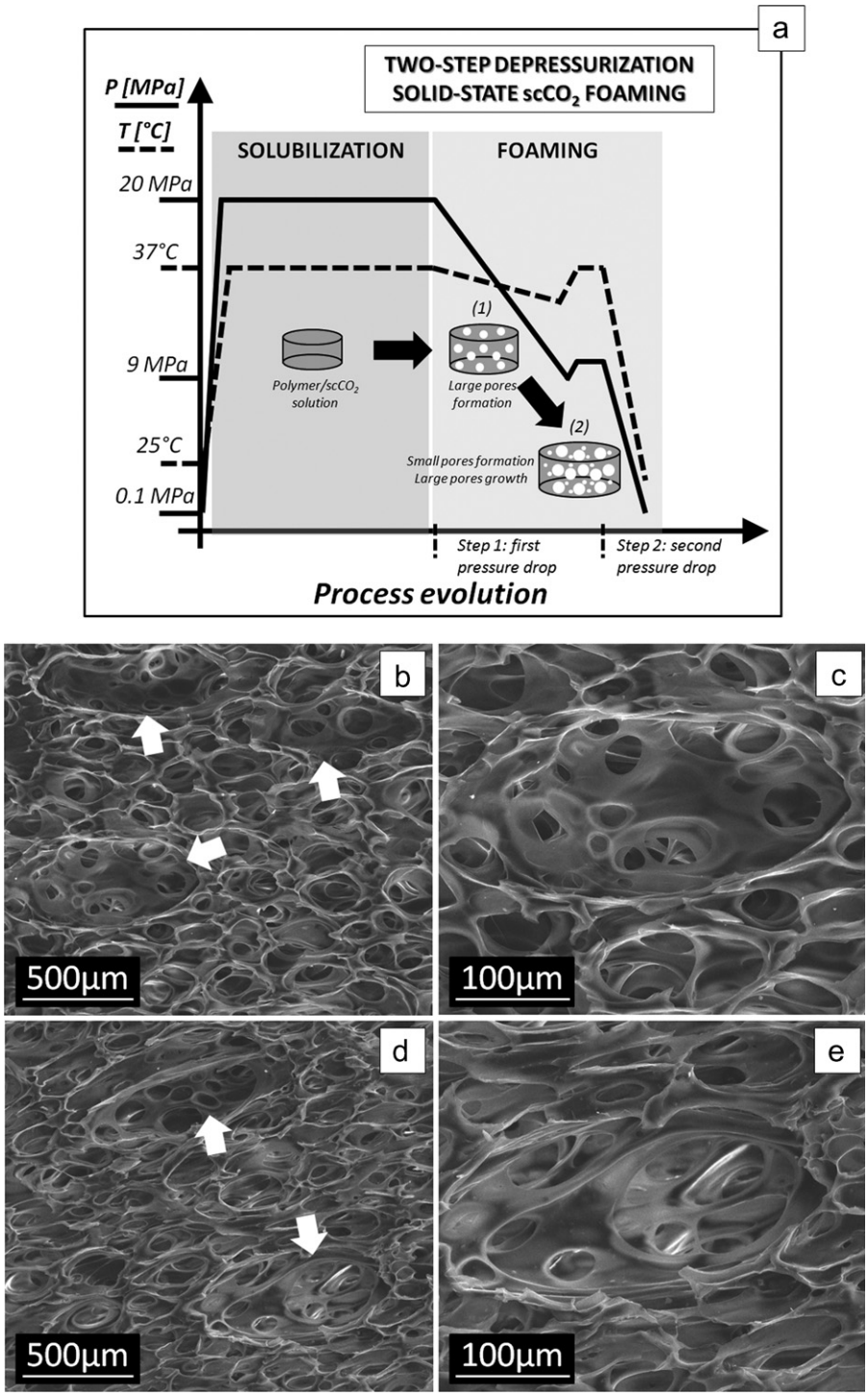

Fig. 9. (a) Evolution of the temperature and pressure of the system during the two-step depressurization foaming process and schematization of the resulting foam's pore structure. SEM microscope images of the (b) and (d) PCL and (c) and (e) PCL-HA foams obtained by the two-step depressurization foaming process. The white arrows of figures (b) and (d) highlighted the macro-pores of the foams.

terized by larger pores if compared to those obtained at 2 and 15 s. Although minor differences were observed on the morphology of the foams as a function of the cooling process for a depressurization time of 2 or 15 s, in the case of the depressurization time of 900 s, the pore size interestingly increased with the decrease of the cooling time (compare Fig. 5g–i). Similar results were also achieved for the PCL-HA nano-composites (inset of Fig. 6), while in this case the presence of the HA particles was clearly evident on the pore walls of the foams (Fig. 6a).

The mean pore size and pore size distribution of the foams were shown in Fig. 7. In agreement with the morphological results of Figs. 5 and 6, the 2 and 15 s depressurization times produced foams with similar mean pore sizes, close to 40 μm. Conversely, when depressurization was performed for 900 s, the mean pore size increased up to six times, in the range from 100 to 250 μm (Fig. 7a and b). Furthermore, these samples evidenced the increase of the pore size with the increase of the cooling rate and, the highest values were observed for the PCL and PCL-HA quenched in liquid N_2.

These results were corroborated by those of the pore size distributions reported in Fig. 7c–f. In particular, minor differences were observed as a function of the thermal history for the PCL and PCL-HA samples foamed at a depressurization time of 2 s (Fig. 7c and d), characterized by pore sizes in the range from 7.5 to 67.5 μm. Conversely, the foams produced at a foaming time equal to 900 s (Fig. 7e and f), evidenced pores in the range from 25 to 425 μm and wider pore size distributions.

Fig. 8 showed the pore density of the PCL and PCL-HA foams of Figs. 5 and 6. The pore density decreased from 10^8 to 10^5 with the increase of the depressurization time from 2 to 900 s. Furthermore, in agreement with the previously reported results, in the case of the highest depressurization time, the slowly cooled samples showed a one order of magnitude higher pore density value if compared to those quenched in liquid N_2.

Our results are in agreement with literature data that highlight the key role of the thermal history and foaming parameters on the pore structure of polymeric foams fabricated by the solid-state $scCO_2$ foaming process [1,24]. For instance, Doroudiani et al. studied the effect of the thermal history on the solid-state foaming of several semi-crystalline polymers, such as polyethylene, polybutylene and polypropylene [1]. They showed that the decrease of the cooling rate produced foams with more irregular pore structures and higher densities. This effect was ascribed to the increase of the fraction of crystallinity of the samples that reduced the solubility and diffusivity of the blowing agent. Similar results were reported by Baldwin et al. for the $scCO_2$ foaming of polyethylene terephthalate [24]. Furthermore, in their work the authors also ascribed this effect to the heterogeneous pore nucleation at the interface between the amorphous and un-plasticized crystalline phases [24]. Interestingly, our results also indicated that the foaming process was affected by the thermal history mainly at a very slow depressurization time. In particular, we observed that, when depressurization was performed for 900 s, the porosity (Fig. 4) and the mean pore size (Fig. 7) increased with the decrease of the cooling time and, the higher values were achieved in the case of the foams prepared starting from the films quenched in liquid N_2 (fast). Conversely, the pore density decreased with the decrease of the cooling time (Fig. 8), again more evident at slow depressurization time. As also reported in literature [13], the decrease of the foaming time reduces the utility of the nucleating agents, by enhancing the homogeneous nucleation rates. Conversely, at high foaming times, the heterogeneous nucleation may be more relevant and, therefore, the crystalline structure mat significantly impact on the pore structure of the foams. Although several works were reported about the melting of PCL under similar $scCO_2$ conditions [18–20], the different foaming behaviour of the samples as a function of the thermal history demonstrated indirectly that the saturation conditions used in this study were unable to completely erase the thermal history of the starting materials. Therefore, this aspect need to be taken into the account in designing PCL and PCL-HA foams with well controlled pore structures.

3.2.2. *Two-step depressurization foaming*

One of the most promising application of the solid-state $scCO_2$ foaming is the design of porous scaffolds for TE. Indeed, the low $scCO_2$ temperature and the absence of organic solvents, potentially harmful to cells and biological tissues, may allow for the simultaneous processing of biomaterials, cells and molecular cues [9–11]. The results of the morphological characterization reported in Figs. 4 and 5 showed that the foams prepared in this study were characterized by rather low pore interconnectivity. This characteristic, coupled with the hydrophobic nature of PCL [14], may hinder the achievement of a sufficient cell and tissue infiltration in three-dimensions. To overcome this limitation, our group has recently demonstrated that PCL scaffolds with bi-modal pore size distributions may improve the ability of transplanted cells to adhere, proliferate and differentiate *in vitro* in three-dimensions [25,26]. To evaluate the feasibility of the solid-state $scCO_2$ foaming process to produce porous PCL and PCL-HA foams with bi-modal pore size distribution and improved TE performances, we performed a preliminary foaming test based on a two-step of depressurization. Although this approach was used to prepare bi-modal polystyrene foams [21,27], in our knowledge there is a lack of investigations reporting the two-step depressurization solid-state $scCO_2$ foaming of PCL. As shown in Fig. 9a, the PCL and PCL-HA samples where saturated with the $scCO_2$ at 20 MPa and 37 °C for 1.5 h and, subsequently the pressure was released to an intermediate pressure of 9 MPa with a high depressurization time, to allow for the formation of large pores. After this step, the system was allowed to re-equilibrate to 37 °C and, finally the pressure was released very fast to induce the nucleation of smaller pores and the growth of the existing ones. The experiments were conducted on the PCL and PCL-HA samples quenched in liquid N_2 due to their enhanced foaming capability, as previously reported.

The morphologies of the PCL and PCL-HA foams are shown in Fig. 9b–e, clearly evidencing the presence of a bi-modal pore structure. In particular, smaller pores, with size in the range from 50 to 100 μm, were homogeneously distributed all around larger pores, characterized by a mean pore size of 500 μm, approximately (white arrows). Interestingly, the analysis of the inner walls of the macropores showed the presence of extensive interconnections, probably originated during the growth of the large pores and the formation of the smaller ones in the second depressurization step.

4. Conclusions

In this study we investigated the solid-state $scCO_2$ foaming of PCL and PCL-HA nano-composite.

The results demonstrated that the control of the thermal history and foaming parameters is essential to design foams with suitable expansion ratios and homogeneous pore structures. Indeed, foams with high controlled morphology, porosity and pore size distributions were achieved by selecting a saturation pressure and temperature of 20 MPa and 37 °C, respectively, and by the modulation of the depressurization time in the range from 2 to 900 s. Furthermore, we reported that the thermal history had a pivotal role on the solid-state $scCO_2$ foaming of PCL and PCL-HA. In particular, when quenched in liquid N_2, the PCL and PCL-HA produced foams with higher porosity, in the range from 75 to 83%, and mean pore size, from 40 to 300 μm, if compared to those prepared from the slowly and intermediate cooled samples.

Finally, by performing a two-step depressurization foaming starting from the PCL and PCL-HA nano-composite samples quenched in liquid N_2, we prepared foams with bi-modal and highly interconnected porosities, therefore opening new routes for the design of porous scaffolds for TE applications.

Acknowledgments

The authors thank Fabio Massa for his support to carry out the experimental activity. This research has been supported by a grant from the Italian Ministry of Health, TISSUENET n. RBPR05RSM2.

References

[1] V. Kumar, N.P. Suh, A process for making microcellular thermoplastic parts, Polymer Engineering and Science 30 (1990) 1323–1329.
[2] D.L. Tomasko, H. Li, D. Liu, X. Han, M.J. Wingert, L.J. Lee, K.W. Koelling, A review of CO_2 applications in the processing of polymers, Industrial and Engineering Chemistry Research 42 (2003) 6432–6456.

[3] A. Salerno, S. Iannace, P.A. Netti, Open-pore biodegradable foams prepared via gas foaming and microparticulate templating, Macromolecular Bioscience 8 (2008) 655–664.
[4] E. Kiran, Foaming strategies for bioabsorbable polymers in supercritical fluid mixtures. Part II. Foaming of poly(ε-caprolactone-co-lactide) in carbon dioxide and carbon dioxide + acetone fluid mixtures and formation of tubular foams via solution extrusion, J. Supercritical Fluids, doi:10.1016/j.supflu.2010.05.004.
[5] A. Salerno, M. Oliviero, E. Di Maio, S. Iannace, Thermoplastic foams from zein and gelatin, International Polymer Processing 5 (2007) 480–489.
[6] E.Y. Lee, G. Ryu, S. Lim, Effects of processing parameters on physical properties of corn starch extrudates expanded using supercritical CO_2 injection, Cereal Chemistry 76 (1999) 63–69.
[7] A. Salerno, S. Zeppetelli, E. Di Maio, S. Iannace, P.A. Netti, Novel 3D porous multiphase composite scaffolds based on PCL, thermoplastic zein and ha prepared via supercritical CO_2 foaming for bone regeneration, Composite Science and Technology 70 (2010) 1838–1846.
[8] A. Salerno, M. Oliviero, E. Di Maio, S. Iannace, P.A. Netti, Design and preparation of m-bimodal porous scaffold for tissue engineering, Journal of Applied Polymer Science 106 (2007) 3335–3342.
[9] H. Tai, M.L. Mather, D. Howard, W. Wang, L.J. White, J.A. Crowe, S.P. Morgan, A. Chandra, D.J. Williams, S.M. Howdle, K.M. Shakesheff, Control of pore size and structure of tissue engineering scaffolds produced by the supercritical fluid processing, European Cells and Materials 14 (2007) 64–77.
[10] P.J. Ginker, J.J.A. Barry, P. Tighe, S.R. Mutch, G. Serhatkulu, R.C.O. Oreffo, S.M. Howdle, K.M. Shakesheff, Mammalian cell survival and processing in supercritical CO_2, PNAS 103 (2006) 7426–7431.
[11] H.M. Woods, M.M.C.G. Silva, C. Nouvel, K.M. Shakesheff, S.M. Howdle, Materials processing in supercritical carbon dioxide: surfactants, polymers and biomaterials, Journal of Materials Chemistry 14 (2004) 1663–1678.
[12] L.M. Mathieu, T.L. Mueller, P. Bourban, D.P. Pioletti, R. Müeller, J.E. Månson, Architecture and properties of anisotropic polymer composite scaffolds for bone tissue engineering, Biomaterials 27 (2006) 905–916.
[13] C. Marrazzo, E. Di Maio, S. Ianace, Conventional and nanometric nucleating agents in poly(e-caprolactone) foaming: crystals vs bubbles nucleation, Polymer Engineering and Science 48 (2008) 336–344.
[14] M.A. Woodruff, D.W. Hutmacher, The return of a forgotten polymer-polycaprolactone in the 21st century, Progress in Polymer Science 35 (2010) 1217–1256.
[15] Q. Xu, X. Ren, Y. Chang, J. Wang, L. Yu, K. Dean, Generation of microcellular biodegradable polycaprolactone foams in supercritical carbon dioxide, Journal of Applied Polymer Science 94 (2004) 593–597.
[16] J. Reignier, R. Gendron, M.F. Champagne, Autoclave foaming of poly(e-caprolactone) using carbon dioxide: impact of crystallization on cell structure, Journal of Cellular Plastics 43 (2007) 459–489.
[17] I. Tsivintzelis, E. Pavlidou, C. Panayiotou, Biodegradable polymer foams prepared with supercritical CO_2–ethanol mixtures as blowing agents, J. Supercritical Fluids 42 (2007) 265–272.
[18] Y. Shieh, H. Yang, Morphological changes of polycaprolactone with high-pressure CO_2 treatment, J. Supercritical Fluids 33 (2005) 183–192.
[19] Z. Lian, S.A. Epstein, C.W. Blenk, A.D. Shine, Carbon dioxide-induced melting point depression of biodegradable semicrystalline polymers, J. Supercritical Fluids 39 (2006) 107–117.
[20] E. Kiran, K. Liu, K. Ramsdell, Morphological changes in poly(3-caprolactone) in dense carbon dioxide, Polymer 49 (2008) 1853–1859.
[21] K.A. Arora, A.J. Lesser, T.J. McCarthy, Preparation and characterization of microcellular polystyrene foams processed in supercritical carbon dioxide, Macromolecules 31 (1998) 4614–4620.
[22] Q. Wu, X. Liu, L.A. Berglund, An unusual crystallization behavior in polyamide 6/montmorillonite nanocomposites, Macromolecular Rapid Communications 22 (2001) 1438–1440.
[23] Z. Xu, X. Jiang, T. Liu, G. Hu, L. Zhao, Z. Zhu, W. Yuan, Foaming of polypropylene with supercritical carbon dioxide, J. Supercritical Fluids 41 (2007) 299–310.
[24] D.F. Baldwin, C.B. Park, N.P. Suh, A microcellular processing study of poly(ethylene terephthalate) in the amorphous and semicrystalline states. Part I: microcell nucleation, Polymer Engineering and Science 36 (1996) 1437–1445.
[25] A. Salerno, D. Guarnieri, M. Iannone, S. Zeppetelli, E. Di Maio, S. Iannace, P.A. Netti, Engineered l-bimodal poly(e-caprolactone) porous scaffold for enhanced hMSC colonization and proliferation, Acta Biomaterialia 5 (2009) 1082–1093.
[26] A. Salerno, D. Guarnieri, M. Iannone, S. Zeppetelli, P.A. Netti, Effect of micro- and macroporosity of bone tissue three-dimensional-poly(e-caprolactone) scaffold on human mesenchymal stem cells invasion, proliferation, and differentiation in vitro, Tissue Engineering: Part A 16 (2010) 2661–2673.
[27] J. Bao, T. Liu, L. Zhao, G. Hu, A two-step depressurization batch process for the formation of bi-modal cell structure polystyrene foams using $scCO_2$, J. Supercritical Fluids 55 (2011) 1104–1114.